Spectroscopy system based on a single quantum cascade laser for simultaneous detection of CO and CO_2*

Min Wei(魏敏)[1,2], Qing-Hao Ye(叶擎昊)[3], Rui-Feng Kan(阚瑞峰)[1], Bing Chen(陈兵)[1], Chen-Guang Yang(杨晨光)[1], Zhen-Yu Xu(许振宇)[1], Xiang Chen(陈祥)[1,2], Jun Ruan(阮俊)[1], Xue-Li Fan(范雪丽)[1], Wei Wang(王薇)[1], Mai Hu(胡迈)[1], and Jian-Guo Liu(刘建国)[1,†]

[1] *Anhui Institute of Optics and Fine Mechanics, Hefei Institutes of Physical Science, Chinese Academy of Sciences, Hefei* 230031, *China*
[2] *University of Science and Technology of China, Hefei* 230022, *China*
[3] *Shanghai Institute of Satellite Engineering, Shanghai* 200050, *China*

(Received 23 February 2016; revised manuscript received 13 April 2016; published online 19 July 2016)

A quantum cascade laser (QCL) based system for simultaneous detection of CO and CO_2 is developed. The QCL can scan over two neighboring CO (2055.40 cm^{-1}) and CO_2 (2055.16 cm^{-1}) lines with a single current scan. The wavelength modulation spectroscopy ($f = 20$ kHz) is utilized to enhance the signal-to-noise ratio. A white cell with an effective optical path length of 74 m is used. The calibration of the sensor is performed and minimum detection limits of 1.3 ppb (1×10^{-9}) for CO and 0.44 ppm (1×10^{-6}) for CO_2 are achieved.

Keywords: infrared absorption spectroscope, quantum cascade lasers, wavelength modulation spectroscopy, greenhouse gas

PACS: 42.55.Px, 42.62.–b, 71.35.Cc **DOI:** 10.1088/1674-1056/25/9/094210

1. Introduction

Carbon monoxide (CO) and carbon dioxide (CO_2) affect the heat balance of the atmosphere and participate in the atmospheric chemistry.[1] CO is an important atmospheric pollutant in the troposphere.[2] CO also serves as an indicator of urban pollution, and its anthropogenic source is mainly the incomplete combustion of hydrocarbon fuels.[3] Moreover, CO can react with O_2 to produce CO_2, therefore it is an indirect greenhouse gas (GHG). CO_2 is the most important anthropogenic GHG. It is the main product of combustion processes and human activities. Its annual emissions had grown by about 80% between 1970 and 2004, from 21 gigatonnes (Gt) to 38 Gt, and accounted for 77% of the total anthropogenic GHG emissions in 2004.[4] Reliable and sensitive detection of atmospheric CO and CO_2 simultaneously is necessary,[5,6] as these measurements can be used to determine their sources, leading to an improved understanding of the carbon cycle and climate change.

Tunable diode absorption spectroscopy (TDLAS) technology is ideally suited for trace gas detection in environment monitoring, industry control, and combustion diagnosis due to its advantages of *in situ*, high sensitivity, non-intrusive, and high selectivity.[7–11] Simultaneous detection of atmospheric CO and CO_2 based on TDLAS has been reported by several research groups.[12–15] Gabrysch *et al.*[12] used a near-infrared laser (1.578 μm) for CO and CO_2 simultaneous detection and the sensitivity was increased by a factor of 15 compared to direct absorption, the minimum detection limit for CO and CO_2 was about 10 ppm (100 torr, 1 m) and 53 ppm (8 torr, 1 m). Engelbrecht[13] reported a compact fiber-optic diode laser spectrometer for the two species measurement around 1580 nm, achieving a detection limit of 5.1 ppm CO and 9.1 ppm CO_2 with a 1 m absorption path length at 80 hpa. Chen[14] developed a system for the detection of CO and CO_2 with two near-infrared lasers (1563.62 nm and 1580.99 nm) and a white cell. A remote laser-based sensor for vehicle CO and CO_2 emission detection was designed with a single laser (1.57 μm).[15] Those researches were all based on the near-infrared spectrum, however, the fundamental absorption lines of most trace gases are in the mid-infrared region.[16] Quantum cascade laser (QCL) is now a perfect mid-infrared light source[17] and it is more suitable for high-sensitive trace gas detection in combination with TDLAS and the wavelength modulation spectroscopy (WMS) technique.[18–20] Recent developments of QCL for simultaneous atmospheric trace gases detection have been reported, such as simultaneous detection of atmospheric CH_4 and N_2O emission fluxes by QCLS (4.5 μm, 7.5 μm, and 7.9 μm),[21] and simultaneous atmospheric N_2O and CO detection by a 4.5 μm QCL.[22] A QCL (7.73 μm) based sensor for simultaneous detection of atmospheric N_2O, CH_4, and H_2O was developed with a Herriot cell at 100 torr.[23] However, using a single QCL for simultaneous measurement of atmospheric CO and CO_2 has rarely been reported.

*Project supported by the National Key Scientific Instrument and Equipment Development Project of China (Grnat No. 2014YQ060537), the National Basic Research Program of China (Grant No. 2013CB632803), the Strategic Priority Research Program of the Chinese Academy of Sciences (Grant No. XDA05040102), and the National Natural Science Foundation of China (Grant No. 41405134).

†Corresponding author. E-mail: jgliu@aiofm.ac.cn

© 2016 Chinese Physical Society and IOP Publishing Ltd

In this paper, we develop a mid-infrared laser sensor for simultaneous measurements of atmospheric CO and CO_2 based on a single 4.85 μm continuous wave QCL (CW-QCL). The appropriate wavelength enables simultaneous multi-species measurements using a single laser, simplifying the sensor system and reducing its cost greatly. Two neighboring CO (2055.40 cm^{-1}) and CO_2 (2055.16 cm^{-1}) absorption lines can be covered in a single QCL wavelength scan. A multiple pass absorption cell with an effective path length of 74 m and the WMS technique are employed to achieve high sensitivity.

2. Theory and absorption line selection

2.1. Basic theory of WMS

The absorption spectroscopy obeys the Beer–Lambert law. When adding a sinusoidal modulation of angular frequency ω to the laser, the time variations of the laser frequency ν and the laser intensity are expressed as

$$\upsilon(t) = \bar{\upsilon} + a\cos(\omega t), \tag{1}$$

$$I(t) = \bar{I}_0[1 + i_1\cos(\omega t + \psi_1) + i_2\cos(n\omega t + \psi_2)], \tag{2}$$

where $\bar{\upsilon}$ is the laser center frequency, α is the frequency modulation amplitude depth, $\bar{I}_0$ is the average laser intensity, i_1 and i_2 are the linear and nonlinear amplitudes of the intensity modulation (normalized by $\bar{I}_0$), and ψ_1 and ψ_2 are the phase shifts between intensity and frequency modulation for linear and nonlinear terms, respectively.

The transmission coefficient τ can be described in terms of a Fourier series[24]

$$\tau(\upsilon(t)) = \sum_{k=0}^{\infty} H_k(\overline{\upsilon}, a)\cos(k\omega t). \tag{3}$$

Combining Eq. (3) with the Beer–Lambert relation, the H terms can be defined as

$$H_0 = \frac{1}{2\pi}\int_{-\pi}^{\pi} \exp\left(-\sum_j S_j(T)\phi_j P X_i L\right) \mathrm{d}\theta, \tag{4}$$

$$H_k = \frac{1}{\pi}\int_{-\pi}^{\pi} \exp\left(-\sum_j S_j(T)\phi_j P X_i L\right) \cos k\theta \,\mathrm{d}\theta, \tag{5}$$

where $S_j(T)$ is the line strength of absorption transition j at temperature T, P is the total pressure, X_i is the mole fraction of absorption species i, L is the path length, and ϕ_j is the lineshape function of transition j. When the absorption is more than 0.1, the H terms can be written as

$$H_0 = \frac{PX_iL}{2\pi}\int_{-\pi}^{\pi}\sum_j S_j(T)\phi_j \mathrm{d}\theta, \tag{6}$$

$$H_k = \frac{PX_iL}{\pi}\int_{-\pi}^{\pi}\sum_j S_j(T)\phi_j \cos k\theta \,\mathrm{d}\theta. \tag{7}$$

In general, a lock-in amplifier can be used to acquire the wavelength modulation $2f$ signal by multiplying the detect signal with the reference sinusoid and applying low-pass filters to separate the $2f$ component and eliminate other components outside the filter band. The $1f$ normalized method is often used in WMS to eliminate the influence of light intensity variations.[25,26] In most cases, i_2 is much smaller than 1, and we assume that the phase shift of the linear intensity modulation is π, then the $1f$-normalized $2f$ amplitude can be simplified to

$$I_{2f-\text{normalized}} \propto S(T)\phi PXL. \tag{8}$$

The absorption gas concentration X can be calculated according to the normalized $2f$ signal $I_{2f-\text{normalized}}$ if the gas temperature, pressure, and optical path are fixed. When the gas temperature changes, the measurement result can be corrected with the $S(T)/S(T_0)$ factor, where T and T_0 represent the measurement and the reference temperatures, respectively.[27]

2.2. Absorption line selection

Two neighboring CO and CO_2 absorption lines need to be selected for simultaneous detection. The absorption lines of CO and CO_2 in the mid-infrared spectral region (2000–4000 cm^{-1}) are shown in Fig. 1 based on the HITRAN database.[28] The absorptions of H_2O and N_2O in the same spectral region are also given, which are the potential interferences. For CO_2 and CO, their strong absorption lines are within the spectral range of 2000–2400 cm^{-1}, while N_2O and H_2O also have absorption lines within the range.

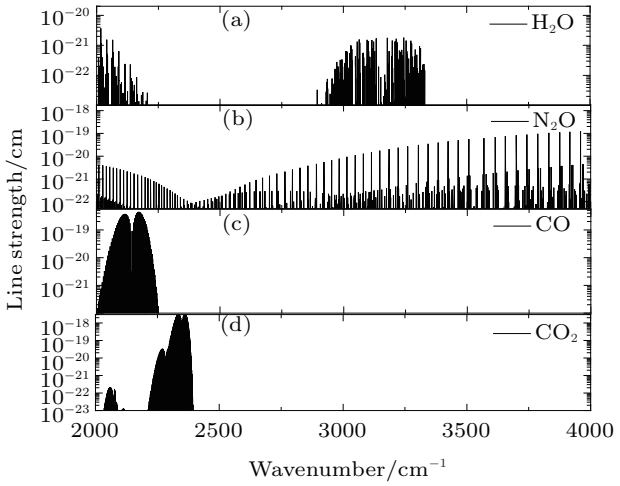


Fig. 1. The absorption line strengths of (a) H_2O, (b) N_2O, (c) CO, and (d) CO_2 at 296 K in the mid-infrared spectra (HITRAN database).

A commercial CW-QCL laser (Alpes laser) covers a wavelength range of 2052–2058 cm^{-1} through tuning its temperature and current. The absorption spectra for 2% H_2O, 380 ppm CO_2, 200 ppb CO, 320 ppb N_2O in air are simulated at 269 K and 250 torr to help to choose the suitable lines, as

shown in Fig. 2. From Fig. 2, the two neighboring lines of CO at 2055.40 cm^{-1} (P21) and CO_2 at 2055.16 cm^{-1} (P28(e)) can be selected, which are fully swept in a single wavelength scan at a fixed temperature (injection current between 140 mA and 165 mA). Their HITRAN parameters are shown in Table 1. Furthermore, the second harmonic signals of different mixture gases of CO and CO_2 at 250 torr are simulated in Fig. 3 to verify that a relative lower pressure (250 torr) can be selected to avoid the spectral interference between CO_2 and CO. From the simulated results, the amplitude of CO (200 ppb) varies ~0.2% when CO_2 changes from 380 ppm to 1000 ppm. Similarly, the amplitude of CO_2 (380 ppm) varies ~0.018% when CO changes from 200 ppb to 3 ppm.

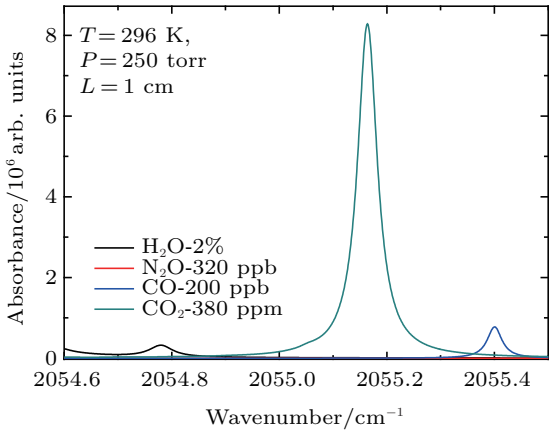


Fig. 2. (color online) The simulated absorption spectra for H_2O, N_2O, CO_2, and CO in air at 296 K and 250 torr based on HITRAN database.

Table 1. Spectroscopic parameters of the selected CO_2 transition at 2055.16 cm^{-1} and CO transition at 2055.40 cm^{-1} at 296 K.

Molecule	υ_0 /cm^{-1}	S /cm^{-2}·atm^{-1}	γ_{air} /cm^{-1}·atm^{-1}	γ_{self} /cm^{-1}·atm^{-1}	n_j
CO_2	2055.16	0.0227	0.069	0.0897	0.78
CO	2055.40	0.62	0.05	0.0543	0.67

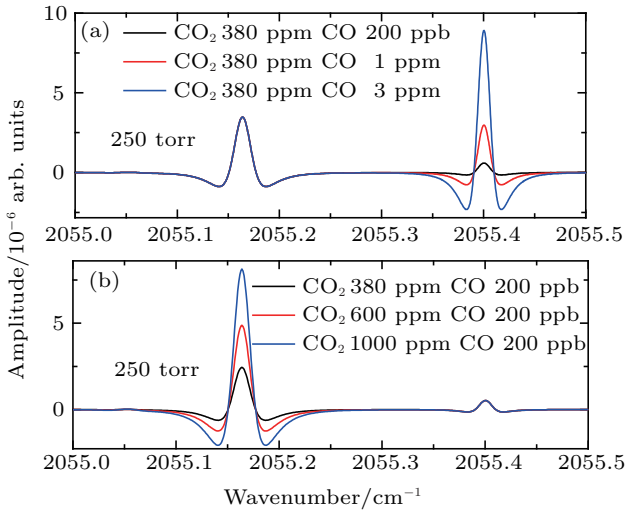


Fig. 3. (color online) The simulated second harmonic signals for different mixtures of CO_2 and CO.

3. Experimental system

The experimental single-QCL-based system is presented in Fig. 4. A continuous wave distributed feedback QCL (Alpes Laser, Switzerland) around 2055 cm^{-1} in a high heat load (HHL) package was used as the light source, with a beam-divergence angle less than 3 mrad. The temperature and the current were simultaneously controlled by a commercial laser controller (LDC 3724B, ILX Lightwave, USA). The mid-infrared light was combined with an aligned visible beam (λ = 650 nm) by a beam splitter ($T > 90\%$ at 4.85 μm, $R > 85\%$ at 650 nm) for aiding the optical alignment. The combined light beam went through two reflect mirrors, then passed into a white multi-pass cell. The cell consists of three spherical mirrors, with a base length of 1 m, which can provide an optical path length of 74 m. The leakage rate of the multi-pass white cell is 0.01 Pa·L/S. The output mid-infrared beam was focused onto an AC thermoelectric cooled mercury cadmium telluride detector (MCT) (PVI-2TE-10.6, Vigo Systems, Poland) using a parabolic mirror (f = 50.4 mm). The detected signal was acquired by a data acquisition (DAQ) card (M2i.4210 PCI 14 bit 20 Ms/s, SPECTRUM, Germany), and then input to a Labview-based lock-in amplifier to extract the $1f$-normalized $2f$ signal.

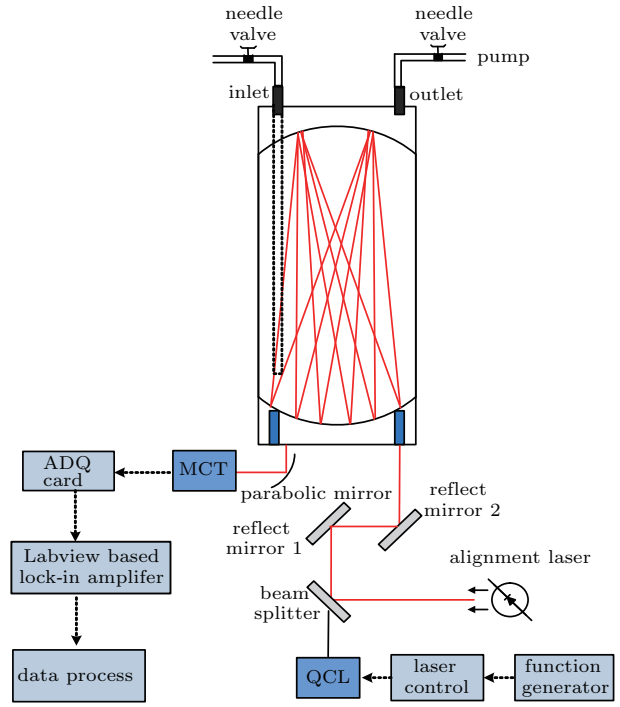


Fig. 4. (color online) Schematic of the experimental apparatus.

The optical path outside the gas cell was about 50 cm, which was 148 times smaller than the inside optical path of 74 m, so the influence of CO and CO_2 in ambient air can be neglected. It is better to make the outside part closed or purge with N_2 particularly for CO_2 detection, because it is easily influenced by human breath in the laboratory.

The two absorption lines were covered by a sweep range of about 0.6 cm^{-1} with a current scan signal of 200 Hz. The modulation depth was optimized, which affects the peak value of the $2f$ signal. The modulation frequency was set at 20 kHz to reduce the low-frequency noise. Under this modulation frequency, the modulation depth varied with the modulation voltage directly, so an appropriate modulation voltage should be selected. The laboratory air flowed into the cell and the needle valves were adjusted to maintain the pressure of 250 torr. The peak value of the $1f$-normalized $2f$ signal is plotted in Fig. 5. As shown in Fig. 5, both the $2f$ peaks of CO and CO_2 reached the maximum with a modulation voltage of about 120 mV, thus this modulation voltage was selected for CO and CO_2 simultaneous detection in the following experiment. The detector signal, the $1f$-normalized $2f$ signal, and the peak values of CO_2 and CO are also given in Fig. 6. The asymmetry of the $2f$ signal in Fig. 6 resulted from the intensity modulation. In Fig. 6, the $1f$-normalized $2f$ signal of CO is different from that of CO_2, this difference perhaps is due to the background effect. Also, the absorbance of CO in the laboratory air was much less than that of CO_2, which would result in different background effects to their $2f$ signals.

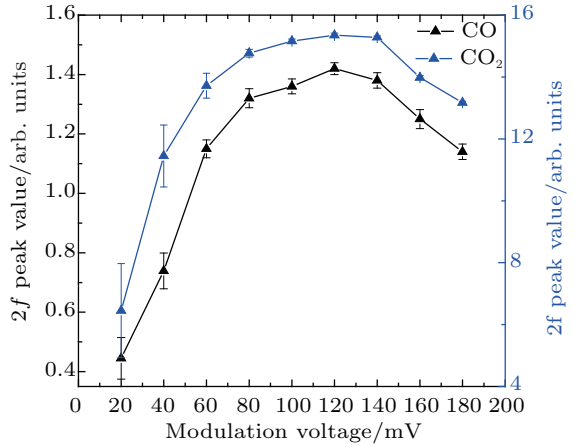


Fig. 5. (color online) The $2f$ peaks of CO and CO_2 in laboratory air at different modulation voltages.

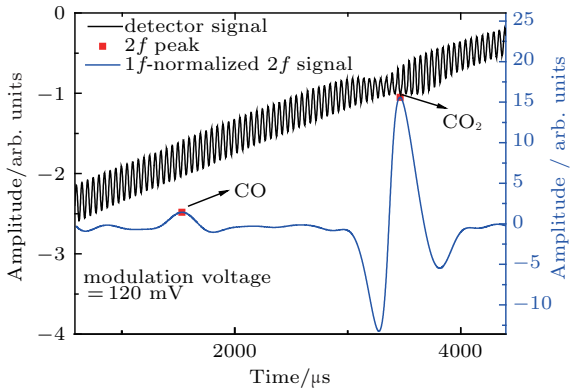


Fig. 6. (color online) An example of detector signal and related $2f$ signal of laboratory air.

4. Experimental results

Several standard gases (Guangming Research & Design Institute of Chemical Industry, with 2% relative uncertainty) with different mole fractions of CO (200 ppb, 500 ppb, 950 ppb, 1.7 ppm, 3.7 ppm) and CO_2 (95 ppm, 257 ppm, 404 ppm, 702 ppm, 1001 ppm) were used for the sensor calibration, and the carrier gas was N_2. During the calibration, these standard gases flowed into the gas cell with the concentration increased. The $2f$ amplitude increased with the concentration of both gases. When each $2f$ peak became stable, the signal was recorded for 20–30 min. The calibration processes of CO and CO_2 are plotted in Figs. 7 and 8. After calibration, a continuous detection of relatively lower standard gas (950 ppb CO, 404 ppm CO_2) was conducted to test the sensor reproducibility, as illustrated in Figs. 7(a) and 8(a).

For CO, the linear fit coefficient of CO is greater than 0.998. For the second 950 ppb CO detection, the average $2f$ amplitude in 30 min is 2.14, and the corresponding value is 2.12 for the first detection in the calibration, so the amplitude difference is 0.02. The related concentration difference between the two stages is 10 ppb (1%). The two differences are small, showing the good reproducibility. Similarly, for CO_2, the linear fit coefficient is greater than 0.99. For two detections of the same concentration of the standard gases, the differences are 0.35 and 15 ppm (3.7%) for the amplitude and the concentration, respectively, which are both relatively small. All these results illustrate a good linear response and reproducibility of the sensor for the detection of CO and CO_2.

In order to test the detection limit and the long-term precision of the experimental system, the laboratory ambient air was closed in the gas cell and continuously measured at 250 torr. An example of the signals is shown in Fig. 9. The continuous detection results of 3000 s are shown in Fig. 10 with 1-Hz sample rate. According to the measurement results, the averaged concentrations of CO and CO_2 are about 1.07 ppm and 509.24 ppm, which are in the normal concentration ranges in atmosphere. During the detection period, the root mean square (RMS) noise is 8 ppb for CO (about 0.7% of the laboratory ambient air level) and 1.78 ppm for CO_2 (about 0.35% of the laboratory ambient air level).

In general, the Allan variance plot is used to seek the optimum integration time and the corresponding minimum detection limit for the system. The Allan variance of the simultaneous detection results is plotted in Fig. 11, which demonstrates that the optimum integration time is about 85 s for the simultaneous detection of CO and CO_2. A minimum Allan deviation of 1.3 ppb for CO ($\sim$ 1‰ of the ambient level) and 0.44 ppm for CO_2 ($\sim$ 0.9‰ of the ambient level) is achieved at the optimum integration time. The high detection limit shows that the system is appropriate for atmospheric monitoring of these two species. With a longer integration time, there is an increase in the Allan Deviation due to the instrumental drifts, including laser wavelength drift, optical drift, and electronic drift.

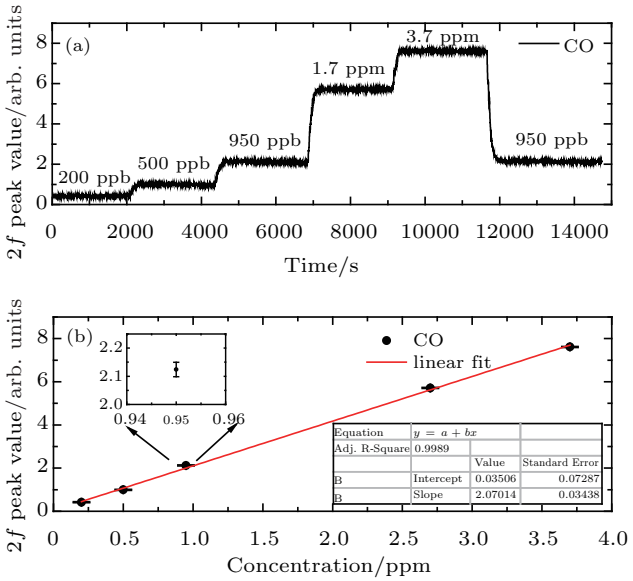


Fig. 7. (color online) Calibration process (a) and calibration results (b) for CO.

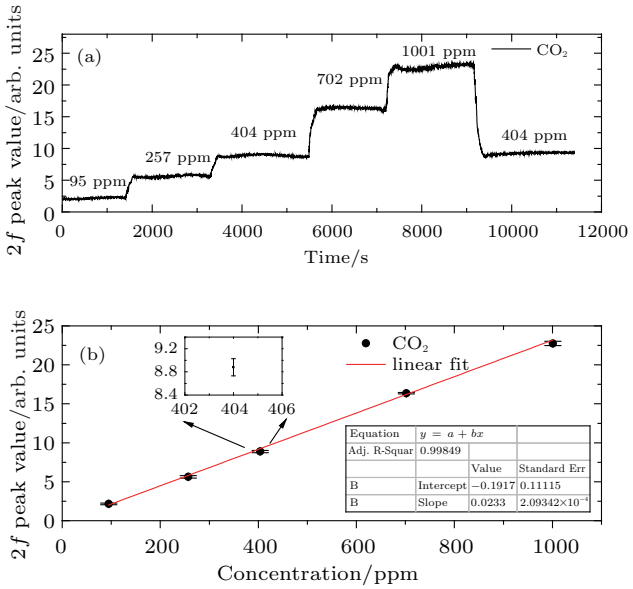


Fig. 8. (color online) Calibration process (a) and calibration results (b) for CO_2.

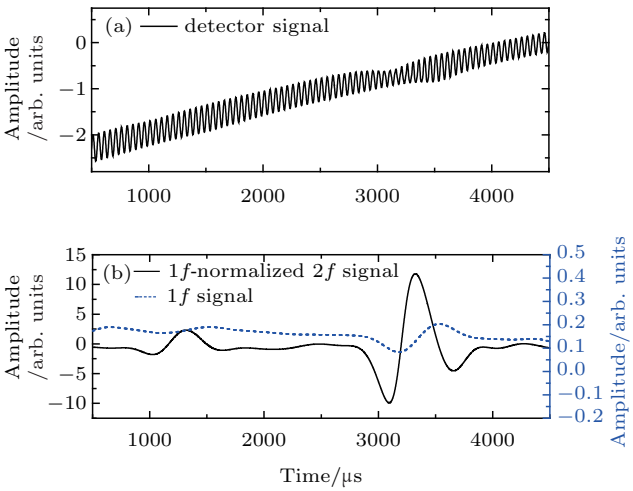


Fig. 9. (color online) An example of the related signals of ambient air: (a) detector absorption signal, (b) normalized $2f$ and $1f$ signals.

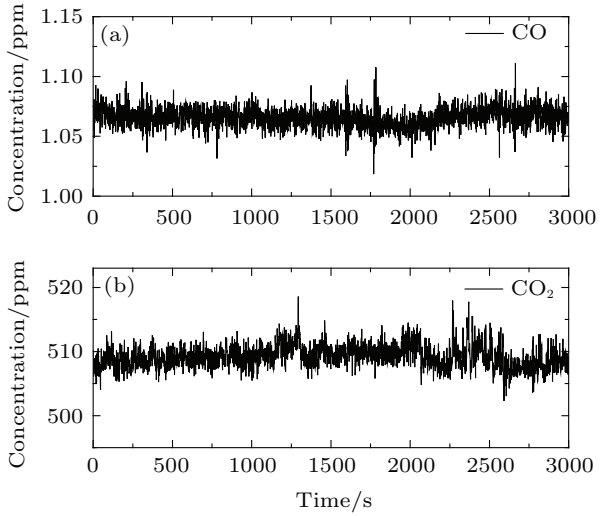


Fig. 10. Continuous measured results of CO (a) and CO_2 (b) in laboratory ambient air for 3000 s.

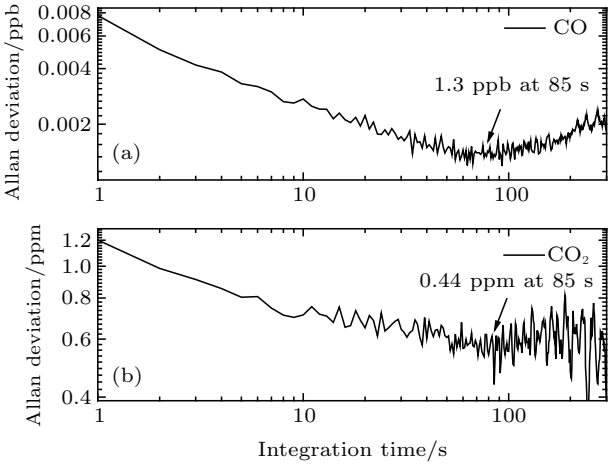


Fig. 11. Allan deviations of CO (a) and CO_2 (b) as a function of integration time.

5. Conclusion

We have developed a single QCL based absorption spectroscopy system for simultaneous detection of atmospheric CO and CO_2 with a 74 m multi-pass cell. Utilization of a single QCL to realize dual-species detection reduced the cost and simplified the experimental configuration. The two neighboring CO (2055.40 cm^{-1}) and CO_2 (2055.16 cm^{-1}) absorption lines were covered within a single wavelength scan. The concentration calibration of the system was performed using standard gases with different concentrations, and the calibration results illustrated a rather good linear response for both CO (200 ppb–3.7 ppm) and CO_2 (95 ppm–1001 ppm). The detection limit and long-term precision of this CO/CO_2 sensor were examined by monitoring the laboratory room air for about 3000 s, and its Allan deviation plots showed that a detection limit of 1.3 ppb for CO and 0.44 ppm for CO_2 can be achieved at 85 s integration time.

References

[1] Tang X Y, Zhang Y H and Shao M 2006 *Atmospheric Environmental Chemistry* (Beijing: Higher Education Press) pp. 56–67 (in Chinese)

[2] Yao L, Liu W Q, Liu J G, Kan R F, Xu Z Y, Ruan J and Dai Y H 2015 *Chin. J. Lasers* **42** 0215003 (in Chinese)

[3] Logan J A, Prather M J, Wofsy S C and Mcelroy 1981 *Journal of Geophysical Research* **86** 7210

[4] Change C 2007 *Synthesis Report. Contribution of Working Groups I, II and III to the Fourth Assessment Report of the Intergovernmental Panel on Climate Change [J].* IPCC 2007

[5] http://www.wmo.int/pages/prog/arep/gaw/documents/Final_GWA_213_web.pdf

[6] Hu Y Y 2012 *Physics* **41** 495

[7] Willer U, Saraji M, Khorsandi A, Geiser P and Schade W 2006 *Optics and Lasers in Engineering* **44** 699

[8] Pan W D, Zhang J W, Dai J M and Song K 2012 *Spectroscopy and Spectral Analysis* **32** 10

[9] Kan R F, Liu W Q, Zhang Y J, Liu J G, Dong F Z, Wang M, Gao S H, Chen J and Wang X M 2005 *Chin. J. Lasers* **32** 1217 (in Chinese)

[10] Chao X, Jeffries J B and Hanson R K 2009 *Measurement Science and Technology* **20** 115201

[11] Xia H, Dong F Z, Wu B, Zhang Z R, Pang T, Sun P S, Cui X, Han L and Wang Y 2015 *Chin. Phys. B* **24** 034204

[12] Gabrysch M, Corsi C, Pavone F S and Inguscio M 1997 *Appl. Phys. B* **65** 75

[13] Engelbrecht R 2004 *Spectrochimica Acta Part A: Molecular and Biomolecular Spectroscopy* **60** 3291

[14] Chen D, Liu W Q, Zhang Y J, Liu J G, Wei Q N, Kan R F, Wang M, Cui Y B and Chen J 2006 *Chin. Phys. Lett.* **23** 2446

[15] Wang T D, Liu W Q, Zhang Y J and Wang M 2007 *Infrared and Laser Engineering* **36** 336 (in Chinese)

[16] Tang Y Y, Liu W Q, Kan R F, Zhang Y J, Chen D, Zhang S and Ruan J 2012 *Chin. Opt. Lett.* **10** 041404

[17] Yan F L, Zhang J C, Yao D Y, Liu F Q, Wang L J, Liu J Q and Wang Z G 2015 *Chin. Phys. B* **24** 024212

[18] Moeskops B W, Cristescu S M and Harren F J 2006 *Opt. Lett.* **31** 823

[19] Kosterev A, Wysocki G, Bakhirkin Y, *et al.* 2008 *Appl. Phys. B* **90** 165

[20] Wysocki G, Bakhirkin Y, So S, Tittle F K, Hill R Q and Fraser M P 2007 *Appl. Opt.* **46** 8202

[21] Mappé I, Joly L, Durry G, Thomas X, Decarpenterie T, Cousin J, Dumelie N, Roth E, Chair A and Grillon P G 2013 *Review of Scientific Instruments* **84** 023103

[22] Tao L, Sun K, Khan M A, Miller D J and Zondlo M A 2012 *Opt. Express* **20** 28106

[23] Cao Y C, Sanchez N P, Jiang W Z, Griffin R J, Xie F, Hughes L C, Zah C and Tillel F K 2015 *Opt. Express* **23** 2121

[24] Li H, Rieker G B, Liu X, Jeffries J B and Hanson R K 2006 *Appl. Opt.* **45** 1052

[25] Klein A, Witzel O and Ebert V 2014 *Rapid Sensors* **14** 21497

[26] Fernholz T. Teichert H and Ebert V 2002 *Appl. Phys. B* **75** 229

[27] Zhang Z R, Wu B, Xia H, Pang T, Wang G X, Sun P S, Dong F Z and Wang Y 2013 *Acta Phys. Sin.* **62** 234204 (in Chinese)

[28] Rothman L S, Gordon I E, Babikov Y, *et al.* 2013 *Journal of Quantitative Spectroscopy and Radiative Transfer* **130** 4